



Effect of H₂S and thiophene on the steam reforming activity of nickel and rhodium catalysts in a simulated coke oven gas stream

Asbel David Hernandez^{a,b,*}, Noora Kaisalo^a, Pekka Simell^a, Marco Scarsella^b

^a VTT Technical Research Centre of Finland, P.O. Box 1000, FI-02044 VTT, Finland

^b University of Rome Sapienza, Department of Chemical Engineering, via Eudossiana 18, 00184, Rome, Italy



ARTICLE INFO

Keywords:

Sulfur poisoning
Coke oven gas
Catalytic steam reforming
Water-gas shift

ABSTRACT

In the present work the impact of H₂S and thiophene on the steam reforming and water-gas shift (WGS) reactions were studied. The activity of three catalysts i.e. Ni/Al₂O₃, Ni/mayenite and Rh/Al₂O₃ was evaluated using an atmospheric fixed-bed lab-scale quartz reactor. A simulated coke oven gas (COG) stream was fed to the reactor. The temperature range studied was 675–900 °C. It was found that the temperature had a significant influence on the degree of poisoning of the catalysts and thus their performance. Regeneration of benzene reforming activity of the poisoned Ni/Al₂O₃ was achieved after exposing the catalyst to up to 200 ppm of H₂S. Rh/Al₂O₃ outperformed the nickel catalysts in the steam reforming of benzene in the presence of thiophene. Ni/mayenite was the only catalyst able to maintain a noticeable WGS activity in the presence of H₂S this result was attributed to the presence of CaO on the surface of this catalyst.

1. Introduction

Coke oven gas (COG) is a hydrogen-rich gas and a by-product of the coal carbonization in steel plants. It has been the subject of intense research in recent years due to its potential and key role in the improvement of the energy efficiency within the steelmaking industry [1–3]. COG can be used as fuel in the steel plant, for example in reheating furnaces or in power plants. Instead of just burning the COG, it could potentially be used for fuel or chemical synthesis or for electricity production in fuel cells.

COG comprises mainly H₂ (55–60 vol-%), CH₄ (23–27 vol-%), CO (5–8 vol-%), N₂ (3–6 vol-%) and CO₂ (less than 2 vol-%) [1]. Besides the main compounds, the raw COG includes a complex matrix of hydrocarbons (tars) and minor constituents such as NH₃, H₂S, organic sulfur compounds, hydrogen cyanide, ammonium chloride and CS₂ [2]. For advanced use of COG these impurities need to be removed. Typically, the cleaning process consists of a series of coolers to reduce the temperature of the gas below 30 °C. During this process, approximately 30% of the initial NH₃ and most of the tar components are removed [2]. Water and tar are transferred to the tar separator for crude tar recovery. In the subsequent gas cleaning steps, different scrubbing processes are used to reduce the content of H₂S, BTX and NH₃ [2]. However, the conventional treatment of COG does not reach the stringent gas quality requirements for chemical synthesis or fuel cells application [4]. Thus,

more advanced cleaning and upgrading is required.

Hydrocarbons in COG can be converted to H₂ and carbon oxides by reforming. Tar reforming technology from biomass gasification gas cleaning [5–8] can be exploited for COG cleaning. Similar to COG, biomass gasification syngas contains tar and sulfur compounds. Sulfur in biomass gasification gas is mainly in the form of H₂S [9]. Typical thiophene concentration in biomass gasification gas is less than 10 ppm (v), usually in the range 1–100 ppb(v) [10]. Whereas in COG, thiophene concentration can reach up to 100 ppm(v) [11]. Thiophenic compounds (e.g. thiophene, alkyl-thiophenes and benzo-thiophene) are the most abundant and stable organic sulfur species present in COG [12]. It is known that H₂S can be readily removed, for example by sorbents or absorbers units, while the organic sulfur compounds are difficult to remove [13]. Industrially, hydrodesulfurization units are used to convert organic sulfur compounds to H₂S. If these compounds could be converted to H₂S in the reformer while converting the hydrocarbons to syngas, it would simplify the cleaning when COG is used for syngas production.

Lakhapatri et al. [14] used TEM-EDS to study the deactivation mechanism caused by thiophene under steam reforming conditions using a Ni-Rh/Al₂O₃ catalyst and suggested that thiophene decomposition occurs primarily on the surface of Ni crystallites, leading to the deactivation of these sites. Moreover, no bulk sulfide formation (neither on Ni nor on Rh) was found on the used catalyst. The common

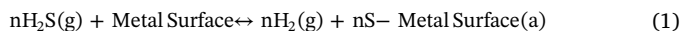
* Corresponding author. Present address: VTT Technical Research Centre of Finland, P.O. Box 1000, FI-02044 VTT, Finland.

E-mail addresses: asbel.hernandez@uniroma1.it (A.D. Hernandez), noora.kaisalo@vtt.fi (N. Kaisalo), pekka.simell@vtt.fi (P. Simell), marco.scarsella@uniroma1.it (M. Scarsella).

assumption that organic sulfur compounds are fully converted to H₂S under reforming conditions finds support in thermodynamics studies [12] as well as in the study conducted by Lu et al. [15]. However Lakshapathi et al. [16] in their study of steam reforming of Jet A spiked with thiophene using a Ni/Al₂O₃ catalyst at 800 °C found unreacted thiophene in the condensate after the first few minutes of the reaction. From the results of Rhyner et al. [17] and Mayne et al. [18], it seems more adequate to state that depending on the reaction conditions, organic sulfur compounds can attain different degrees of conversion and desulfurization.

The interaction of H₂S with nickel surfaces involves a number of steps including molecular adsorption, dissociative chemisorption, surface diffusion and reconstruction of the sulfur adlayer into a two-dimensional nickel/sulfur compound [19]. Moreover, the structure and stoichiometry of sulfur adsorbed on nickel are complex functions of temperature, H₂S concentration, sulfur coverage, and pretreatment [20].

Eq. (1) represents the reversible sulfur chemisorption reaction on transition and noble metals.



This reaction is highly exothermic [21], thus increasing the temperature of the catalyst will shift the chemisorption equilibrium to the left-hand side of Eq. (1) and from a thermodynamic point of view, it is possible to regenerate or alleviate the poisoning effect of sulfur on the catalyst by increasing the temperature. This approach has been adopted in many studies dealing with H₂S poisoning of active metal for the steam reforming reactions [22–24]. Conclusions about the renewability of the active sites of the catalyst on lab-scale reactors by increasing the temperature cannot be straightforwardly extrapolated to industrial-scale processes due to diffusion restrictions [25].

In this work, the impact of H₂S and thiophene on the performance of the steam reforming of CH₄ and benzene as a tar model compound in a simulated COG stream using two typical steam reforming catalysts namely nickel and rhodium supported on alumina was studied. In addition, it was also tested a novel mayenite-supported nickel catalyst in the reforming of benzene. The effect of sulfur on the water gas shift reaction activity was investigated with the nickel-based catalysts in a hydrocarbon-free stream.

2. Experimental section

2.1. Experimental set-up and sampling

The laboratory-scale tests were conducted in an atmospheric plug-flow reactor (Fig. 1). The detailed description can be found from Tuomi et al. [7]. The quartz reactor used in the experiments had an inner diameter of 10 mm equipped with a thermocouple pocket of 4 mm. The temperature was measured from the centre of the catalyst bed by a K-type thermocouple. All the lines that were in contact with the gas/vapor streams were passivated to avoid biased results due to interaction with H₂S.

A continuous gas analyzer (Sick Maihak S710) was used to determine the CO, CO₂, H₂ and O₂ content in dry gas. All hydrocarbons were analyzed by an online GC Agilent 7890A equipped with two columns and two FID detectors. For the experiments carried out without thiophene a GS-GASPRO column (30 m, 0.32 mm ID, film 20 μm) was used to measure hydrocarbons from CH₄ to C₅, whereas benzene concentration was measured using a HP-5 column (30 m, 0.32 mm ID, film 25 μm). In the presence of thiophene, all compounds were separated using a HP-5 column (30 m, 0.32 mm ID, film 25 μm). Calibration of the continuous gas analyzer was performed every two weeks.

For some selected tests, gas bag samples were collected to analyze the thiophene outlet concentration and other sulfur containing compounds. The analysis was made by a GC (Agilent 7890A) equipped with a flame photometric detector (FPD).

2.2. Experimental conditions and test procedure

The model COG composition used in the tests is presented in Table 1. Benzene (Merck, > 99.7%) was used as tar model compound. For the study of the impact of thiophene on the steam reforming reaction, a mixture of thiophene 5 wt.% (Merck, > 99.0) and benzene 95 wt.% (Merck, > 99.7) was used. As sulfur chemisorption has a strong dependence on temperature, benzene and thiophene reforming was studied without methane in the gas to ensure close-to-isothermal catalyst bed conditions. In addition to reforming experiments, the effect of H₂S on the water gas shift (WGS) reaction was studied without hydrocarbons in the feed. The total gas flow rate was 2.1 l/min in all the experiments. The GHSV calculated considering the effective bed volume inside the quartz reactor was 76 000 h⁻¹.

The experiments were conducted in the temperature range 650–900 °C. Several experiments were carried out in duplicate and the average value is presented in the figures of the result section.

All experiments were run for at least 2 h. To evaluate the time required for the establishment of the sulfur chemisorption equilibrium in the entire catalyst bed, sulfur was added after steady state conditions were reached. The GHSV was kept constant by replacing the corresponding sulfur flow with nitrogen and vice versa.

Considering that the scope of the present manuscript was a deeper understanding of the effect sulfur on the performance on the catalyst, the experimental conditions were carefully chosen to limit as much as possible the carbon deposition. To minimize the carbon deposition issue, the minimum steam to carbon (S/C) ratio was 3 and when methane was not included in the feed stream the ratio was 85. Moreover, the addition of C₂ + hydrocarbons was avoided as it's well known that their presence enhances whisker carbon formation. Furthermore, after reaction there was not any visual evidence of carbon formation.

Thermal decomposition tests of the mixture of benzene and thiophene were carried out with SiC particles. In those experiments the volume of the bed, the total inlet flow rate and the inlet composition were the same as in the catalytic steam reforming of the mixture benzene-thiophene.

2.3. Catalysts and catalyst characterization

The catalysts used in the experiments were Ni/Al₂O₃, Rh/Al₂O₃ and Ni/mayenite. The latest was synthesized using the auto-combustion method using glycine as oxidizer, nickel loading was 20 wt.%. The detailed synthesis procedure can be found elsewhere [8]. Ni/Al₂O₃ and Rh/Al₂O₃ were prepared by wet impregnation. The nickel loading was 10 wt.% and the rhodium loading was 1.5 wt.%.

In each test 1.2 g of catalyst were used with particle size of 0.2–0.3 m. To achieve uniform bed temperatures, the catalysts were diluted with SiC to 1:1 vol ratio. The particle size of SiC was 0.30–0.35 m.

The nickel catalysts were characterized by hydrogen chemisorption and X-ray diffraction analyses (XRD). XRD analyses were performed with a PANalytical X'Pert PRO MPD Alpha-1 diffractometer using Cu Kα1 radiation (45 kv and 40 mA) in continuous scan mode in the range 10°–70° (2θ) and a step size of 0.0131°. The diffractograms were analyzed with the EVA software.

Temperature programmed reduction (TPR) measurements before the H₂ chemisorption analysis were performed under a 5 vol-% H₂/argon flow from room temperature to 800 °C with a 10 °C/min rate. A thermal conductivity detector (TCD) was used to measure the H₂ consumption. Ni/mayenite and Ni/Al₂O₃ showed a unique and pronounced trough at 750 °C and 400 °C respectively, while Rh/Al₂O₃ displayed a small trough at 230 °C with a shoulder at 180 °C. The pulse chemisorption technique was carried out at 25 °C using 0.1 g of catalyst under a 5 vol-% H₂/argon flow.

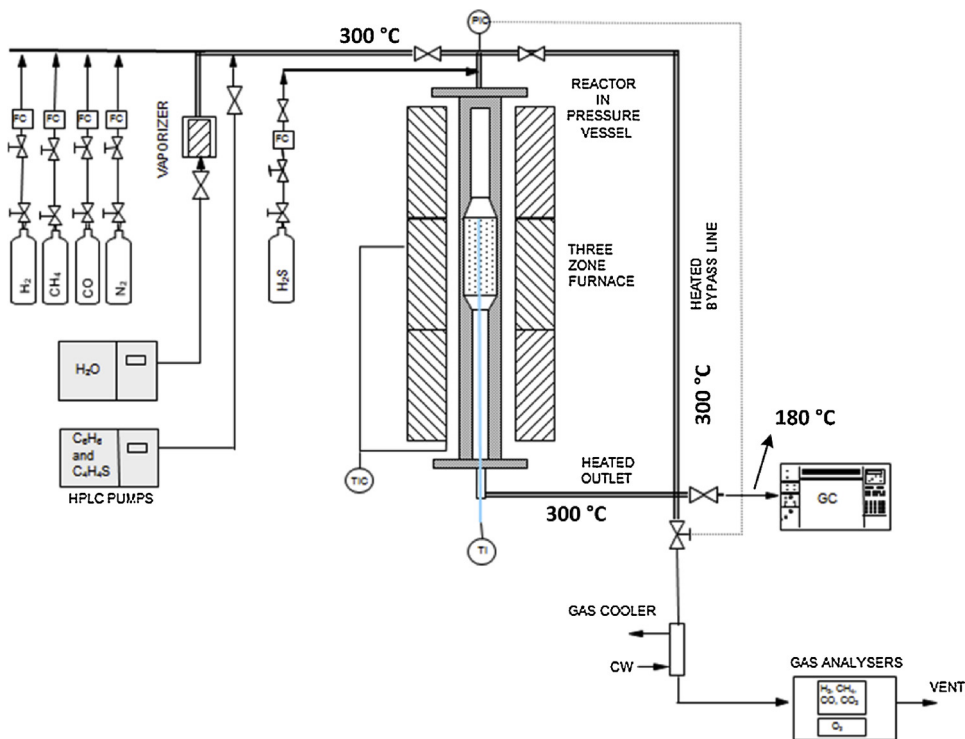


Fig. 1. Atmospheric plug-flow reactor.

Table 1

Inlet composition used in the experiments.

	Dry gas composition					Wet basis		
	CO vol.%	CH ₄ vol.%	H ₂ vol.%	N ₂ vol.-%	H ₂ S ppm(v)	C ₄ H ₆ S ppm(v)	C ₆ H ₆ ppm(v)	H ₂ O vol. %
SR CH ₄ + Bz	5.3	35.9	50.0	8.8	0-200	0	1000	48.7
SR CH ₄ + Bz + Th	5.3	35.9	50.0	8.8	0	50	950	48.7
SR Bz	5.3	0	50.0	44.7	0-200	0	1000	48.7
SR Bz + Th	5.3	0	50.0	44.7	0	50	950	48.7
WGS	5.3	0	50.0	44.7	0-100	0	0	48.7

Bz: Benzene. Th: thiophene.

2.4. Calculation methods

2.4.1. Sulfur coverage (θ_s)

Sulfur coverage on the nickel catalysts was calculated using Eq. (3) proposed by Alstrup et al. [26] derived from a Temkin-like isotherm. Alstrup et al. [26] measured sulfur chemisorption isobars for a Ni/MgAl₂O₄ catalyst in the temperature range 500–1000 °C and H₂S/H₂ ratio range 7–50 ppm. They concluded that up to 90% of saturation the results were well described by Eq. (2) with $\Delta H^\circ = -289 \text{ kJ mol}^{-1}$, $\Delta S^\circ = -19 \text{ J mol}^{-1} \text{ K}^{-1}$ and $\alpha = 0.69$

$$\frac{P_{\text{H}_2\text{S}}}{H_2} = \exp \left[\frac{\Delta H^\circ(1 - \alpha\theta_s)}{RT} - \frac{\Delta S^\circ}{R} \right] \quad (2)$$

Thus, resulting in Eq. (3)

$$\theta_s = 1.45 - 9.53 \times 10^{-5} T + 4.17 \times 10^{-5} T \ln \left(\frac{P_{\text{H}_2\text{S}}}{P_{\text{H}_2}} \right) \quad (3)$$

2.4.2. Elemental balances and conversions

Atomic balance calculations were performed based on the inlet and outlet stream compositions measured by the online GC and the continuous gas analyzer. The total and dry flow rate at the reactor outlet were calculated from the carbon and oxygen balances, while the dry gas

flow rate at the inlet was set by the mass flow meters. It should be noted that in the absence of CH₄, the increase in the outlet flow rate was negligible (less than 1%) and therefore did not have a strong effect in the benzene or thiophene conversions calculations.

Benzene, thiophene and methane conversions were calculated from Eq. (4).

$$X_i = \frac{\dot{F}_{i,\text{IN}} - \dot{F}_{i,\text{OUT}}}{\dot{F}_{i,\text{OUT}}} 100\% \quad (4)$$

where X_i is the conversion of the hydrocarbon; $\dot{F}_{i,\text{IN}}$ and $\dot{F}_{i,\text{OUT}}$ are the inlet and outlet molar flow rates of the hydrocarbons, respectively.

3. Results

3.1. Catalyst characterization

3.1.1. XRD

The XRD analysis of the nickel catalysts is presented in Fig. 2. Identification of the chemical species was done correlating the data to powder diffraction file (PDF) numbers. The Ni/Al₂O₃ showed narrow peaks for nickel and alumina phases (Fig. 2B). The Ni/mayenite spectra displayed the characteristic peaks of mayenite and metallic nickel in addition peaks corresponding to CaO were also present (Fig. 2A). XRD characterization for the Rh/Al₂O₃ was not performed.

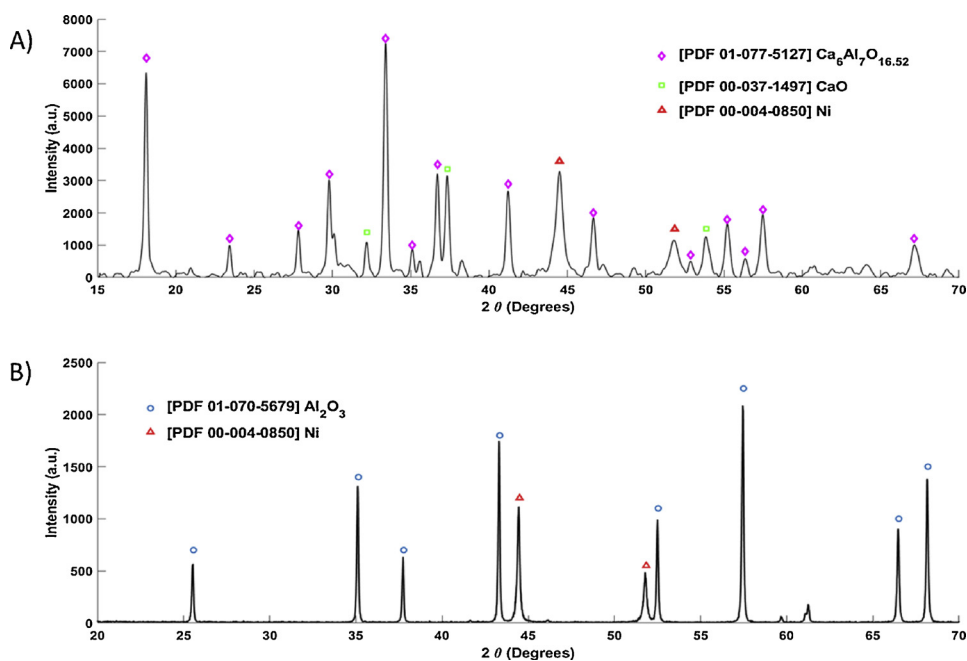


Fig. 2. Diffractograms of the reduced catalyst. A) Ni/mayenite. B) Ni/Al₂O₃.

3.1.2. Catalyst properties based on H₂ chemisorption analysis

The catalyst properties based on the hydrogen chemisorption analysis are presented in Table 2. The metal surface area was computed assuming a H/metal = 1:1 stoichiometry. The Rh/Al₂O₃ showed the highest dispersion of active metal and the largest metal surface area. The sulfur capacity at the saturation (S_0) of the catalysts is also listed in Table 2. The calculation was done assuming that 440 µg S/m² Ni is equivalent to 1 m²/g Ni as proposed by Rostrup-Nielsen [27] and the metal surface area. The sulfur capacity was calculated to have an approximate value of the maximum sulfur uptake of the catalyst bed used in the experiments. It should be kept in mind that S_0 calculation for the Rh/Al₂O₃ may be less accurate because the equivalence was obtained using a nickel catalyst. The total sulfur capacity of the catalyst bed was calculated from the sulfur capacity at saturation, the theoretical mass content of the metal in the catalyst and the total mass of catalyst in the bed, i.e. 1.2 g.

3.2. Thermodynamic calculations

Thermodynamic calculations based on the minimization of the Gibbs free energy were performed using the software Aspen Plus® and HSC Outokumpu. No thermodynamic limitations were found for the conversion of benzene even at the lowest temperature used in the experiments (i.e. 650 °C). In the case of methane, the calculations showed 4 vol. % on a dry-basis at 650 °C. It was seen from the thermodynamic results that the WGS reaction was far from equilibrium in all the reactions conditions studied. Furthermore, it was confirmed that thiophene has a large thermodynamic driving force toward H₂S formation in the conditions studied in this work [18].

Table 3

Sulfur coverage and the corresponding benzene conversion using Ni/Al₂O₃ at different H₂S concentrations at oven temperatures of 700 °C, 800 °C and 900 °C.

Oven T. (°C)	H ₂ S (ppm(v dry basis))	Cat T (°C)	θs	X _{C6H6} %	H ₂ S/H ₂ (x10 ⁻⁶)
900	25	887	0.86	94	50
	50	888	0.89	89	100
	75	888	0.91	82	150
	100	888	0.93	76	200
	200	889	0.96	52	400
	10	785	0.87	53	20
	25	786	0.91	26	50
	50	787	0.94	14	100
	75	787	0.96	9	150
	100	788	0.97	6	200
800	200	787	1.00	3	400
	10	683	0.93	4	20
	25	683	0.96	3	50
700					

3.3. Sulfur coverage (θs)

The calculated sulfur coverage along with the corresponding benzene conversion are displayed in Table 3. The sulfur coverage was calculated only for the experiments performed without methane and using the Ni/Al₂O₃ catalyst. The outlet H₂ concentration was used to calculate the H₂S/H₂ ratio. The H₂S/H₂ partial pressure ratio stayed well below the bulk sulfide formation at the working temperatures studied [27]. The sulfur coverages spanned from 0.86 to 1 and hence all values were relatively close to one. It is important to mention that during the benzene steam reforming reaction carried out with the fresh catalysts i.e. before feeding H₂S, the conversion values were always

Table 2
Catalysts properties estimated from the H₂ chemisorption characterization.

	Metal dispersion (%)	Metal surface area (m ² g metal ⁻¹)	Active particle diameter (nm)	Sulfur capacity at saturation (µg g metal ⁻¹)	Total sulfur capacity of the catalyst bed (µg)
Ni/Al ₂ O ₃	0.4	2.6	255	1144	137
Ni/Mayenite	0.7	4.5	148	1980	475
Rh/Al ₂ O ₃	9.3	41.0	12	18040	324

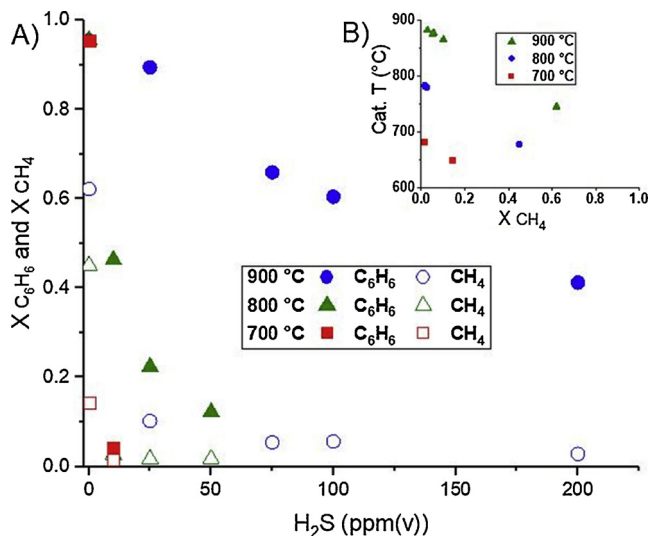


Fig. 3. A) Impact of the H_2S concentration on the benzene and methane steam reforming activity of Ni/Al_2O_3 at the oven temperatures of $700\text{ }^\circ C$, $800\text{ }^\circ C$ and $900\text{ }^\circ C$. B) Temperature measured from the centre of the catalyst bed as a function of methane conversion.

higher than 94% and the temperature of the catalyst was very close to the set oven temperature. Thus, in all the experiments conducted at the same oven temperature, the catalyst temperature was nearly similar regardless the different H_2S concentrations used as can be seen from Table 3 and Fig. 4B.

3.4. Effect of H_2S on steam reforming

The impact of the H_2S concentration on the methane and benzene steam reforming activity of Ni/Al_2O_3 is shown in Fig. 3A. Complete conversion of methane was not achieved at any of the temperatures studied. Considering the results of thermodynamic calculations, it can be concluded that the system did not reach the equilibrium when methane was present in the feed. Moreover, when the oven temperature was $900\text{ }^\circ C$, the effect of the H_2S concentration seemed to be stronger on methane conversion than on benzene conversion. Nevertheless, at

$900\text{ }^\circ C$ the moles of carbon converted in the case of methane were higher than for benzene, for all the H_2S concentrations studied. Almost complete deactivation i.e. conversion of methane close 1%, of the catalyst towards methane steam reforming was observed with 10 ppm(v) H_2S working at oven temperatures $\leq 800\text{ }^\circ C$. It is noteworthy that in the experiments carried out without H_2S , the catalyst bed temperature dropped considerably with respect to the set oven temperature, which can be seen from Fig. 3B. This was particularly evident when the oven temperature was $900\text{ }^\circ C$ and it can be attributed to the endothermic nature of the steam reforming of methane.

For the whole range of operating conditions studied, the chemisorption of H_2S on the catalysts and thus their deactivation was very fast (few seconds), observed from the instantaneous temperature increase of the catalyst bed during the experiments with methane. After a rapid drop in conversion and fast temperature increment, a steady state was reached, and the conversions of methane and benzene remained stable during the rest of the test without signs of further deactivation or activity loss.

Furthermore, formation of any light hydrocarbons during the experiments was not observed, except for small amounts of methane c.a. 240 ppm(v) that was formed at $700\text{ }^\circ C$ in the absence of both H_2S and CH_4 in the feed.

The tests conducted without methane in the feed (Fig. 4A) resulted in a similar benzene conversion versus H_2S concentration curves as the ones reported in Fig. 3A. During those experiments, the catalyst bed temperature was close to the set oven temperature, only 2–5 °C higher than without H_2S . Compared to the results with methane, the most noticeable differences were found in the experiments carried out at the oven temperature of $900\text{ }^\circ C$ when the H_2S concentration was ≥ 75 ppm (v). At these conditions, the benzene conversion was c.a. 15% points higher in the absence of methane. It should be mentioned that during the benzene steam reforming experiments the catalyst bed temperature was $888\text{ }^\circ C$ i.e. 10 °C higher than the temperature measured during the tests conducted when methane was also present.

The CO_2 concentration measured at the outlet of the reactor was around 2–3 vol-% during the benzene steam reforming without H_2S in all the temperatures. However, when H_2S was present, the CO_2 concentration dropped to almost zero very fast i.e. less than 5 min after the introduction of H_2S . This behavior was observed for all the temperatures and H_2S concentrations studied, even when benzene conversion was high.

The ability of the catalyst to regenerate its C_6H_6 and CH_4 steam reforming activity from the sulfur poisoning was studied with Ni/Al_2O_3 , the results are showed in Fig. 5. The regeneration experiments consisted

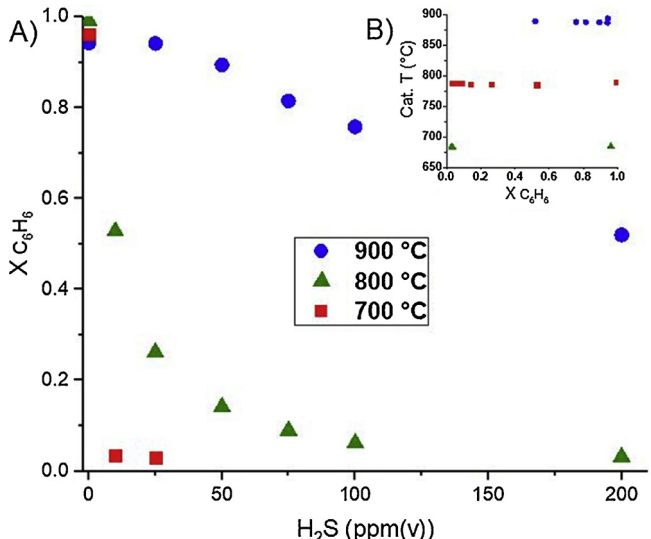


Fig. 4. A) Impact of H_2S on the benzene steam reforming activity of Ni/Al_2O_3 in the absence of methane at set oven temperatures of $700\text{ }^\circ C$, $800\text{ }^\circ C$ and $900\text{ }^\circ C$. B) Temperature measured from the centre of the catalyst bed as a function of benzene conversion.

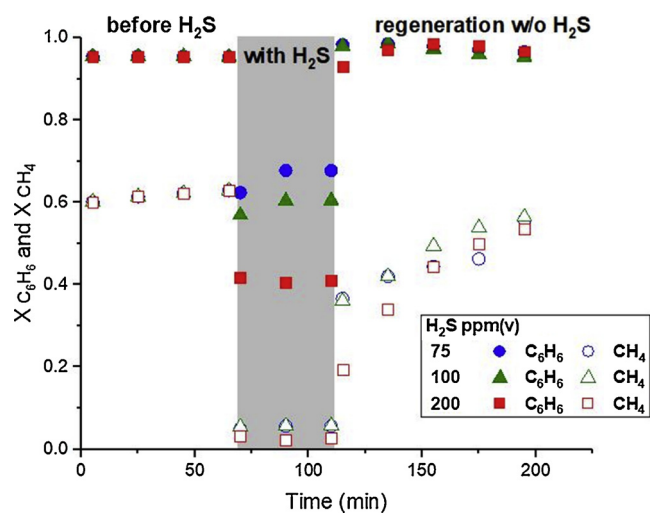


Fig. 5. Regeneration of the benzene and methane steam reforming activity of Ni/Al_2O_3 after exposure to H_2S at $900\text{ }^\circ C$.

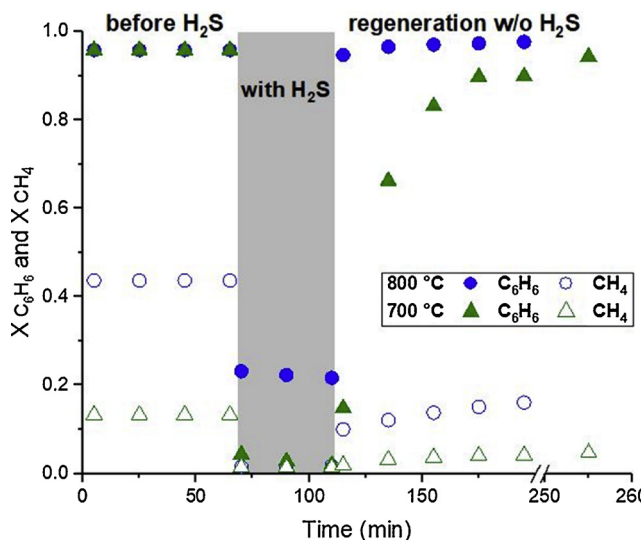


Fig. 6. Regeneration of the benzene and methane reforming activity of Ni/Al₂O₃ at 800 °C and 700 °C after exposure to 25 ppm(v) and 10 ppm(v), respectively.

of three phases: initial activity, poisoning phase and regeneration. All the phases were done at the same oven temperature. The regeneration from H₂S poisoning was done by setting the H₂S in the inlet stream to zero. The catalyst regained rapidly (ca. 5 min) its initial benzene steam reforming activity for the whole range of H₂S concentrations studied. When the catalyst had been exposed to H₂S concentrations of ≤ 100 ppm(v), the methane conversion increased from zero to 37% in the first 5 min of regeneration and after this first increment the methane conversion continued to rise steadily, although at a slower rate. On the other hand, regeneration of the methane steam reforming activity of the catalyst after exposure to 200 ppm(v) of H₂S was slower at the beginning of the experiment although it reached the same level of conversion as in the 100 ppm(v) test after 60 min time on stream. Complete regeneration of the methane steam reforming activity of the catalyst was not achieved at any of the H₂S concentrations studied as can be seen in Fig. 5.

Fig. 6 depicts the results of the experiments carried out at 800 °C and 700 °C using 25 ppm(v) and 10 ppm(v) H₂S in the feed, respectively. The used H₂S concentrations were chosen to have similar sulfur coverages as in the tests carried out at 900 °C and 75 ppm(v) H₂S (Table 3). At 800 °C, the benzene steam reforming activity was recovered completely, and the recovery was only slightly slower than in the regeneration experiments at 900 °C. In contrast, at 700 °C the observed regeneration of benzene reforming activity was much slower reaching similar conversion values as in the fresh catalyst after 255 min. The methane conversion, on the other hand, reached only 36% of the initial conversion at both temperatures at the end of the tests. The catalyst temperature at the end of the regeneration experiments was 746 °C and 667 °C when the oven temperature was 800 °C and 700 °C, respectively, these values were higher than the initial ones, which were 680 °C and 650 at 800 °C and 700 °C respectively.

3.5. Effect of thiophene on the steam reforming of C₆H₆

To evaluate and compare the activity of the catalysts on the conversion of thiophene, Ni/mayenite, Ni/Al₂O₃ and Rh/Al₂O₃ were tested at different temperatures. In addition, thermal conversion of benzene and thiophene was tested with SiC. The results are presented in Table 4. With SiC, the conversion of benzene was negligible even when the SiC bed temperature was 895 °C. However, thiophene conversion reached 72% at 895 °C, whereas at the lowest temperature, i.e. 686 °C, 16% conversion was attained. With the Rh/Al₂O₃, complete conversion

Table 4

Conversion of thiophene and benzene and CO₂ volume fraction in outlet gas for the catalysts studied.

Bed material	T oven (°C)	T cat (°C)	X C ₆ H ₆ (%)	X C ₄ H ₄ S (%)	CO ₂ before feeding C ₆ H ₆ (dry vol-%)	CO ₂ during C ₄ H ₄ S exposure (dry vol-%)
SiC	900	895	1	72	0.0	0.0
	800	790	0	41	0.0	0.0
	700	686	0	16	0.0	0.0
Rh/Al ₂ O ₃	900	873	97	100	3.0	0.2
	800	775	43	100	2.7	0.0
	700	673	6	100	2.3	0.0
Ni/Al ₂ O ₃	900	875	85	100	2.2	0.2
	800	780	9	100	2.3	0.0
	700	675	0	83	2.4	0.0
Ni/mayenite	900	885	81	100	3.0	2.4
	800	784	11	100	3.3	1.8
	700	679	4	86	2.7	0.4

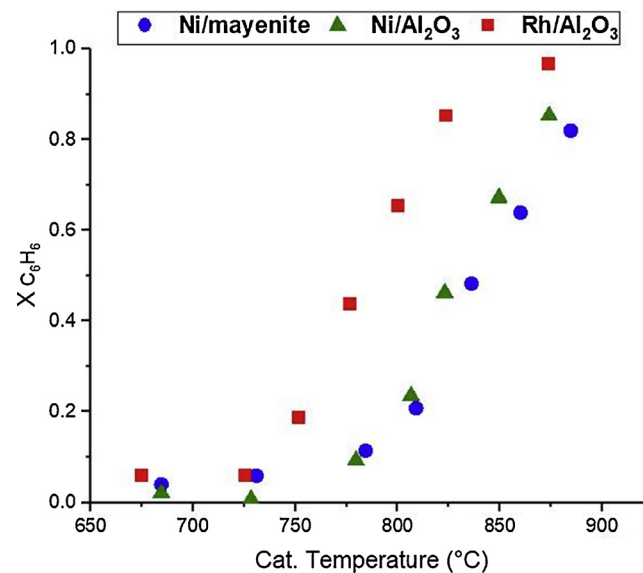


Fig. 7. Benzene conversion as function of the catalyst temperature for the Ni/Al₂O₃, Ni/mayenite and Rh/Al₂O₃ catalysts in the presence of thiophene.

of thiophene was attained at all the temperatures, whereas with the nickel catalysts incomplete conversion of thiophene was observed at temperatures ≤ 680 °C.

Fig. 7 shows the effect of the catalyst bed temperature on the benzene steam reforming conversion in the presence of thiophene for the three catalysts studied. Both nickel catalysts exhibited similar trends, whereas the rhodium catalyst showed higher activity values at temperatures ≥ 775 °C. Moreover, a similar decrease in the activity was noticed for the three catalysts at temperatures ≤ 725 °C. Every point in the curve represents the steady state observed conversion at every temperature and hence different sulfur coverages are expected along the curve. Nevertheless, as the thiophene concentration was kept constant and the H₂ concentration at the outlet was similar for all the experiments conducted at each temperature, the sulfur coverage should be also similar for the three catalysts at a fixed temperature.

As in the experiments with H₂S, the presence of thiophene in the feed affected CO₂ formation on the catalysts as can be seen from Table 4. With Ni/Al₂O₃ and Rh/Al₂O₃ the CO₂ formation was inhibited in the presence of thiophene at all the temperatures studied, except for a small amount of CO₂ observed when the oven temperature was 900 °C. On the other hand, in the case of Ni/mayenite significant amounts of CO₂ were measured at all the temperatures, reaching the highest concentration at the highest temperature.

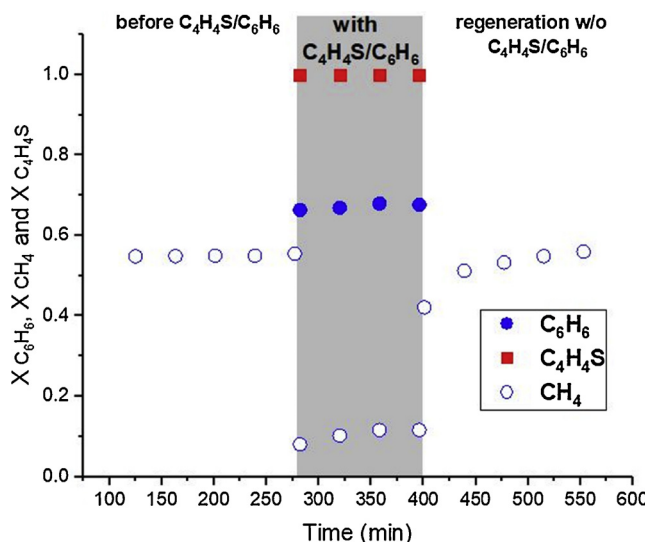


Fig. 8. Regeneration of the methane steam reforming activity of Ni/Al₂O₃ after exposure to benzene-thiophene mixture at 900 °C.

The sulfur compounds formed in the thermal decomposition experiments were analyzed at an oven temperature of 800 °C. The analysis confirmed that almost all the converted thiophene was found as H₂S with a small amount of carbonyl sulfide, i.e. 1 ppm(v). The sulfur-containing compounds were analyzed also in the experiments with Ni/Al₂O₃ and Rh/Al₂O₃ in similar conditions as the thermal decomposition experiment. In both cases, complete thiophene conversion was observed. As in the thermal experiment, COS (1 ppm(v)) was the only other sulfur compound found, the rest was converted to H₂S. Since no hydrocarbons were detected at the exit of the reactor except benzene which was fed along with thiophene, it was concluded that the catalysts converted the hydrocarbon part of thiophene into CO, CO₂, H₂.

The regeneration of Ni/Al₂O₃ after exposure to 50 ppm(v) of thiophene was tested with CH₄ but without benzene in the feed since benzene and thiophene were fed together. The catalyst regeneration was followed by CH₄ conversion. The regeneration experiment was conducted at 900 °C. The results are shown in Fig. 8. The regeneration behavior was similar as in the experiments with ≤100 ppm(v) of H₂S, i.e. a fast recovery of the activity in the first five minutes followed by a steady increase at a slower rate. Moreover, benzene conversion (68%) during 50 ppm (wet basis) thiophene poisoning was identical to the conversion obtained in with the 75 ppm(v) (dry basis) of H₂S. The catalyst temperature before and during the exposure to the thiophene-benzene mixture was 773 °C and 871 °C respectively and the end of the regeneration it returned to 773 °C.

3.6. Effect of H₂S on the Water gas shift reaction (WGS)

To have a better understanding of the effect of H₂S on the water gas shift activity of the nickel catalysts, a series of experiments were conducted with only H₂, CO, H₂S and steam. The Ni/mayenite catalyst was clearly more active in WGS reaction than Ni/Al₂O₃ as can be seen from the higher CO₂ concentrations in Fig. 9. The same could be also observed during the experiments with thiophene, in Table 4.

The WGS regeneration tests were carried out at three different temperatures. An H₂S concentration of 100 ppm(v) was used during the poisoning period. As can be seen from Fig. 9, the Ni/mayenite catalyst exhibited an enhanced sulfur poisoning resistance towards the WGS reaction with respect to the Ni/Al₂O₃ catalyst and this feature becomes more evident as the temperature was increased. When the oven temperature was set to 700 °C both catalysts showed negligible regeneration, whereas at 900 °C fast and complete recovery of the WGS activity was achieved with both nickel catalyst. Equilibrium CO₂ vol-% (dry)

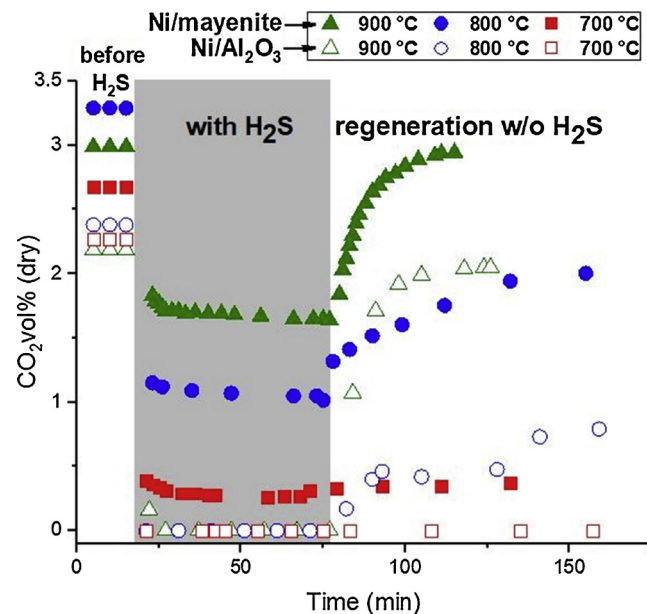


Fig. 9. Regeneration of the water gas shift activity of Ni/Al₂O₃ and Ni/mayenite after exposure to 100 ppm(v) of H₂S at oven temperatures of 700 °C, 800 °C and 900 °C.

values calculated using the Gibbs reactor on Aspen Plus® were 4.9 vol-%, 4.6 vol-% and 4.4 vol-% at 700 °C, 800 °C and 900 °C respectively. Hence, the WGS reaction did not reach equilibrium at any temperature and with any of the catalysts used. Moreover, during tests with the inert material at similar operating conditions the WGS did not take place at any temperature.

4. Discussion

4.1. Effect of H₂S on the steam reforming activity

The effect of H₂S on the steam reforming activity was studied with the Ni/Al₂O₃ catalyst. Fig. 3A showed that benzene conversion was less affected by the presence of H₂S than methane conversion. This was particularly evident when the oven temperature was ≥ 800 °C. Similar results have been reported in the literature [24,28].

When comparing benzene conversion when methane was fed to the reactor (Fig. 3A) to the conversion values when methane was not present in the feed (Fig. 4A), it is noteworthy how the benzene conversion at 700 °C and 800 °C is almost identical with increasing H₂S concentration i.e. the presence of methane had no effect on the benzene conversion. On the contrary, differences between the benzene conversion versus H₂S concentration curves were observed at 900 °C, particularly when the H₂S concentration was ≥ 75 ppm(v).

A possible explanation for the observed results can be that at high catalyst temperature (≥ 870 °C) and when the active sites for steam reforming conversion are exiguous due to high sulfur coverage, competitive reactions between methane and benzene for the scant active sites could take place, hence reducing the benzene conversion with respect to the tests carried out in the absence of methane. However, Jess [29] did not observe any competitive reactions between benzene and methane during steam reforming of simulated COG under sulfur-free conditions using a commercial nickel catalyst. As a possible explanation for the absence of competitive reactions he proposed that methane and benzene were adsorbed weakly and hence did not influence the catalytic conversion of each other. Nonetheless, it must be borne in mind that in the present work the content of methane in the gas was an order of magnitude higher than that of benzene. Therefore, the nickel active sites requirement for methane decomposition must likely be higher

than the nickel sites needed for benzene decomposition, if the same types of sites are required [30].

On the other hand, when the temperature was $\leq 800\text{ }^\circ\text{C}$, it can be argued that differences in thermal stability of C_6H_6 and CH_4 (benzene being thermally less stable [31]) and also possible differences in activation energy required to reform those compounds, contributed to the absence of competitive reactions i.e. methane steam reforming is more demanding than the benzene reforming and hence did not affect the steam reforming rate of the aromatic compound.

4.2. Poisoning and regeneration of $\text{Ni}/\text{Al}_2\text{O}_3$ catalyst

The sulfur capacity of the catalyst bed can be used to estimate the timeframe for the establishment of a new steady state after poisoning of the fixed bed of powder form catalysts in the presence of H_2S . The sulfur mass flow was 15–294 $\mu\text{g}/\text{min}$ when the H_2S concentration was 10–200 ppm(v). When comparing the inlet sulfur mass flow to the sulfur capacity of the catalyst bed (Table 2), it can be noticed that the catalyst bed is saturated with sulfur in 0.5–9 min, if all the sulfur is adsorbed on the catalyst. The time frame is in line with the observed deactivation time. Similar results are obtained with Ni/mayenite and $\text{Rh}/\text{Al}_2\text{O}_3$. Further calculations with the same method but using the data of Ashrafi et al [22] who used 110 g of a commercial nickel-based catalyst in pellet form (diameter = 2–7 mm) did not yield coherent values compared to the timeframe of deactivation observed by the authors [22]. Underestimation of one order of magnitude of the poisoning response using the estimated total sulfur capacity of the fixed used by Ashrafi et al [22] was likely due to mass transfer limitations. In the present study the benzene reforming activity of $\text{Ni}/\text{Al}_2\text{O}_3$ did not drop once the initial decay was observed. This outcome evidenced the difference between the sulfur coverage which considers the equilibrium of sulfur chemisorption and the total surface sulfur capacity of the catalyst bed which does not change with temperature or H_2S concentration.

The observed fast deactivation times, regardless of the H_2S concentration, detected by the rapid increase in the catalyst bed temperature could be ascribed to the fact that sulfur binds strongly and preferably to the nickel surface sites with the highest activity for steam reforming, namely edges and steps [32–34]. Therefore, even the lowest concentration of H_2S i.e. lowest sulfur coverage, can deactivate the sites responsible for the major share of activity of the catalyst and consequently it will cause an immediate effect on the catalyst temperature. The remained steam reforming activity could be due to the sulfur-free terrace sites [33] and/or due to formation of new sites for the steam reforming [35].

The regeneration experiments showed that the initial benzene conversion was more easily recovered than methane conversion. As stated in the result section complete regeneration of the steam methane reforming activity of the catalyst was not achieved at any of the H_2S concentrations studied. This was especially the case at the temperatures of 700 and 800 $^\circ\text{C}$ (Fig. 6). Ashrafi et al [22] studied the regeneration of a Ni-based catalyst at 700 $^\circ\text{C}$ after poisoning the catalyst with 108 ppm (v) H_2S . The authors attained 45% methane steam reforming recovery of the initial activity after 6 h time on stream, whereas in our study the methane conversion reached 36% of initial conversion during the regeneration time of around 2 h. The low recovery of the methane steam reforming activity at lower temperatures could be ascribed to the inability to remove enough sulfur from the surface of the catalyst due to the high binding energy of the sulfur chemisorbed on nickel, which requires higher temperatures for the break of the nickel-sulfur bond. However, it is also possible that the catalyst structure may have undergone an irreversible change during the poisoning experiments [36]. Even though the regeneration of the catalyst activity in benzene steam reforming was fast in the present study extrapolation of the obtained results to industrial-scale applications cannot be done straightforwardly. On the industrial-scale steam reformers both the equilibration

time and the regeneration time of the catalysts even at high temperatures is difficult and slow because the elution process is subject to diffusion restrictions and even without diffusion restrictions, the sulfur leaving the reactor in a hydrogen stream will decrease exponentially with time [25].

4.3. Correlation between sulfur coverage and benzene conversion

Sulfur coverage of nickel catalyst was calculated by Eq. (3). The use of this equation is very popular at typical steam reforming temperatures, mainly because it is easy to apply and have a relatively broad temperature and $\text{H}_2\text{S}/\text{H}_2$ range of validity. Compared to the conditions of this study, the sulfur chemisorption carried out by Alstrup et al. [26] were done using a 13 wt.% nickel supported on a magnesium-aluminum spinel (4.4×4.4 mm cylinders) catalyst with a nickel surface area of $0.3\text{ m}^2/\text{g}$ catalyst. Moreover, at high sulfur coverage the subsurface sulfur atoms become stable relative to surface sulfur [37–39] and this effect is not taken into account by using Eq. (3).

The effect of temperature on benzene conversion can be compared at similar surface coverages of sulfur. (Table 3). For example, at $\theta_s = 0.91$ the benzene conversion was 26% and 82% at 800 $^\circ\text{C}$ and 900 $^\circ\text{C}$, respectively. Without sulfur in the feed the benzene conversion was close to 100% at both temperatures. In contrast, when H_2S was fed to the reactor, even though the sulfur coverage was similar, the activity of the catalyst at 800 $^\circ\text{C}$ was clearly lower than at 900 $^\circ\text{C}$. It should be noted that this high sulfur coverage is at the upper limit of the applicability range of Eq. (3). It is also possible that some nickel ensembles with high activation energy become active only at 900 $^\circ\text{C}$. Likewise, the reconstruction of the nickel surface caused by sulfur chemisorption at high temperatures could have triggered the formation of new sites for benzene reforming [35]. The hypothesis of reconstruction of the nickel surface by adsorbed sulfur finds considerable support in the literature [32,40,41]. According to Maurice et al [32] with increasing sulfur coverage the sulfur phase forms islands, which preferentially develop at step edges on the upper terraces and eventually completely cover the terraces. The Ni atoms then diffuse from the terrace sites to the step edges to reduce the surface stress caused by the sulfur chemisorption thus allowing the formation of a less dense Ni plane [32] and probably this diffusion triggers the formation of new active sites for the reforming reaction.

4.4. Steam reforming of thiophene containing COG

Catalytic thiophene conversion was complete or $\geq 80\%$, already at the lowest temperature used as shown in Table 4. The thermal conversion of thiophene ranged from 17% at the lowest temperature of 675 $^\circ\text{C}$ to 72% at 895 $^\circ\text{C}$. Therefore, the catalytic activity had the biggest share in the total conversion of thiophene. Poisoning of the catalyst by sulfur was evidenced by the low benzene conversion at low temperatures.

Fig. 7 shows that $\text{Rh}/\text{Al}_2\text{O}_3$ has a higher sulfur resistance than the Ni catalysts and this difference was most noticeable when the bed catalyst temperature was c.a.780 $^\circ\text{C}$. In the presence of sulfur, the activity of the alumina supported catalysts can be directly related to the active metal as alumina do not interact with sulfur under reducing conditions at temperatures $\geq 700\text{ }^\circ\text{C}$ [24]. Moreover, since the sulfur content in the inlet feed is not enough to form the bulk metal sulfide at the used temperature range [42], the obtained results cannot be explained by the higher stability of the bulk Ni-sulfide than the bulk Rh-sulfide. An X-ray absorption near edge structure spectroscopy (XANES) study conducted by Chen et al. [43] showed that there are different sulfur species present on Rh and Ni catalysts after the steam reforming of normal paraffins doped with 3-methylbenzothiophene at 800 $^\circ\text{C}$. According to Chen et al. [43] metal sulfide and organic sulfide are the dominant sulfur species on the Ni catalyst, whereas sulfonate and sulfate predominate on the Rh catalyst. Therefore, they postulated that

different sulfur chemistry on Ni and Rh catalysts can likely be the reason for their different sulfur tolerance. Along the same line, the results obtained in the present study could be ascribed to different sulfur chemistry. In that case, the sulfur species predominant on the Rh catalyst seems to be less poisoning for the steam reforming reactions than the species present on the nickel catalyst as was presented by Maxted [44]. The observed similar benzene conversion values for the three catalysts tested at ≤ 725 °C do not agree with the hypothesis of different sulfur species present on the rhodium catalyst, probably, at this low temperature both rhodium and nickel active sites formed surface sulfides or the poisoning effect of the sulfate species on the rhodium catalyst is as strong as the sulfide species on the nickel catalysts at ≤ 725 °C. The hypothesis of the formation of sulfides rather than sulfates on the Rh clusters supported on CeO₂ under reforming conditions is not supported by the findings of Lee et al [45]. The authors [45] concluded that a simple thermodynamic driving force cannot explain the formation of sulfates on Rh₄/CeO₂ (111) catalysts after conducting a density functional theory (DFT) study.

Moreover, a previous study by Rodriguez and Hrbek [46] using well-defined structures pointed out that the tendency of Rh to lose its electrons upon sulfur adsorption is lower than most transition metals, this feature translates in fewer changes in the d population of Rh which remains available to interact with reactants and intermediates species [46,47]. Therefore, it is also reasonable to relate the strong sulfur tolerance of Rh/Al₂O₃ at temperatures ≥ 775 °C with the strong resistance of Rh to the sulfur-induced electron withdrawal.

As shown in Table 4 and Fig. 7, similar benzene steam reforming activity in the presence of thiophene was obtained for both nickel catalysts in spite of the differences in nickel loading, active particle diameter, support, metal surface area, sulfur capacity (Table 2) and interaction with the support which was deduced from the TPR analysis. Hence, in the case of nickel catalysts, the benzene steam reforming activity in the presence of thiophene was probably determined solely by the uncovered, non-poisoned, active sites in the catalysts, i.e. the sulfur surface coverage was similar despite the differences in total surface sulfur capacity. It is conceivable that after the establishment of sulfur equilibrium, comparable number and type of active nickel sites were present on both catalysts.

Regeneration after exposure to thiophene showed similar trends as those found in the regeneration tests after exposure to H₂S. This result was expected as it was observed that almost complete conversion of thiophene to H₂S was achieved at temperatures ≥ 730 °C.

4.5. Effect of sulfur on the water gas shift reaction

The water gas shift activity of the catalysts was evaluated based on CO₂ formation. Table 4 shows that when thiophene was present in the feed, the WGS activity of Ni/Al₂O₃ and Rh/Al₂O₃ was negligible compared to the activity of Ni/mayenite. In the case of Ni/Al₂O₃ and Rh/Al₂O₃ catalysts CO₂ formation was completely inhibited in the presence of thiophene, except at the highest temperatures close to 900 °C. In the case of Ni/mayenite the decrease in the WGS activity in the presence of thiophene was less pronounced. This result is unexpected considering the similar benzene steam reforming activity showed by both nickel catalysts in the presence of thiophene and the even higher activity of the Rh/Al₂O₃ (Fig. 7).

Therefore, if the higher obtained benzene conversion (in the presence of thiophene) in the case of Rh/Al₂O₃ was due to the presence of more shielded sulfur species, it can be concluded that the sulfonate and sulfate species are as toxic as the sulfide species for the WGS reaction. Furthermore, according to Karayaka et al [48], the favoured WGS path at high temperatures (≥ 800 °C) is the direct oxidation of adsorbed CO and O species. Both CO adsorption on the active metal sites and oxygen migration from the support-metal interface are suppressed by the presence of sulfur species [21,49–51]. Accordingly, it is surmise that the WGS activity at the high temperatures studied is more sulfur-sensitive

than the steam reforming of benzene on the Rh/Al₂O₃.

The difference between nickel catalysts towards sulfur poisoning was further studied with WGS experiments. The sulfur-resistance of the Ni/mayenite catalyst compared to the Ni/Al₂O₃ is clearly illustrated in Fig. 9. One reason behind the higher sulfur tolerance of Ni/mayenite catalyst could be the ability of mayenite to adsorb sulfur and protect active nickel site as was presented by Li et al. [52]. However, in the study of Li et al. [52] the Ni/mayenite showed higher activity than Ni/Al₂O₃ only until the saturation of mayenite.

Another explanation for the WGS activity of the Ni/mayenite catalyst in the presence of H₂S is the existence of residual CaO in the catalyst as confirmed by XRD analyses (Fig. 2A). Muller et al. [53] found that at 800 °C CaO had similar water gas shift activity than the Fe₃O₄, a known catalyst for this reaction. Therefore, it is reasonable to correlate the water gas shift activity of the Ni/mayenite to the presence of active CaO sites on the surface of the catalyst. In addition to the catalytic WGS activity of CaO, the sulfur adsorption capacity of CaO is known from the literature [54–56]. However, sulfur binds more strongly to nickel than CaO; the heat of adsorption of sulfur on CaO is 3 times lower than on nickel [57]. Thus, it is possible that the nickel in this case served as a sulfur guard for the active sites of CaO. Moreover, Heesink and Swaaij [58] found that CaO reaction with H₂S was hindered by the presence of CO₂, H₂ and CO in the temperature range of 500 and 700 °C. Hence, the presence of CO₂, CO and H₂ could have inhibited the adsorption of sulfur on the CaO active sites leaving them free to catalyze the WGS reaction. The increasing trend of CO₂ formation with temperature suggested that in the studied conditions the WGS reaction was far from the equilibrium (as confirmed by equilibrium calculation) and therefore was limited by kinetics. In the present study, the activity of the mayenite in the water gas shift reaction was not verified.

5. Conclusions

The effect of sulfur compounds on the steam reforming activity of CH₄ and C₆H₆ on Ni/Al₂O₃ in a simulated COG stream was studied. It was shown that temperature significantly influenced the poisoning effect of H₂S. As the temperature was decreased the poisoning effect increased in agreement with the exothermic nature of the sulfur chemisorption equilibrium.

After the initial poisoning the catalyst activity stayed stable. Moreover, the poisoning of the catalyst was fast in all the conditions studied and the timeframe for the establishment of a new steady state after poisoning was close to the calculated time needed to reach the total sulfur capacity of the catalyst bed. During the regeneration tests, the initial benzene conversion was restored in less than 5 min. On the other hand, the methane reforming regeneration process was slower

Above 800 °C, thiophene was completely converted with all the catalysts. Thermal conversion of thiophene was appreciable i.e. 42% at 800 °C. In all the experiments, the sulfur-containing products from thiophene were mainly H₂S with traces of COS. Ni/Al₂O₃ and Ni/mayenite showed similar benzene steam reforming activity versus temperature in the presence of thiophene despite the differences in the catalyst properties. Rh/Al₂O₃, on the other hand, outperformed both nickel catalysts especially at temperatures ≥ 775 °C in the presence of thiophene. Interestingly, both Ni/Al₂O₃ and Rh/Al₂O₃ catalysts lost completely their WGS activity in the presence of thiophene, even when the C₆H₆ conversion was high.

Fast (≤ 5 min) and complete WGS activity deactivation were observed for Ni/Al₂O₃. Regeneration of the catalyst activity was possible only at 900 °C. Ni/mayenite, on the other hand, exhibited a remarkable sulfur WGS activity tolerance and this feature was enhanced as the temperature was increased. This result was ascribed to the presence of CaO in the surface of the Ni/mayenite catalyst.

Declaration of Competing Interest

The authors declare that they have no known competing financial interests or personal relationships that could have appeared to influence the work reported in this paper.

Acknowledgments

This project has received funding from the Fuel Cells and Hydrogen 2 Joint Undertaking under grant agreement No 700300. This Joint Undertaking receives support from the European Union's Horizon 2020 research and innovation programme and Hydrogen Europe and N.ERGHY.

References

- [1] J.M. Bermúdez, A. Arenillas, R. Luque, J.A. Menéndez, An overview of novel technologies to valorise coke oven gas surplus, *Fuel Process. Technol.* 110 (2013) 150–159, <https://doi.org/10.1016/j.fuproc.2012.12.007>.
- [2] R. Razzaq, C. Li, S. Zhang, Coke oven gas: availability, properties, purification, and utilization in China, *Fuel*. 113 (2013) 287–299, <https://doi.org/10.1016/j.fuel.2013.05.070> Review article..
- [3] M.T. Johansson, M. Söderström, Options for the Swedish steel industry - Energy efficiency measures and fuel conversion, *Energy*. 36 (2011) 191–198, <https://doi.org/10.1016/j.energy.2010.10.053>.
- [4] L.J. Bonville Jr., C.L. DeGeorge, P.F. Foley, R.R. Lesieur, J.L. Preston Jr., D.F. Szydłowski, Method for Desulfurizing a Fuel for Use in a Fuel Cell Power Plant, 6,159,256 (2000).
- [5] P. Simell, I. Hannula, S. Tuomi, M. Nieminen, E. Kurkela, I. Hiltunen, N. Kaisalo, J. Kihlman, Clean syngas from biomass. Process development and concept assessment, *Biomass Convers. Biorefinery*. 4 (2014) 357–370, <https://doi.org/10.1007/s13399-014-0121-y>.
- [6] N. Kaisalo, P. Simell, J. Lehtonen, Benzene steam reforming kinetics in biomass gasification gas cleaning, *Fuel*. 182 (2016) 696–703, <https://doi.org/10.1016/j.fuel.2016.06.042>.
- [7] S. Tuomi, N. Kaisalo, P. Simell, E. Kurkela, Effect of pressure on tar decomposition activity of different bed materials in biomass gasification conditions, *Fuel*. 158 (2015) 293–305, <https://doi.org/10.1016/j.fuel.2015.05.051>.
- [8] B. de Capriatis, M.P. Bracciale, P. De Filippis, A.D. Hernandez, A. Petrucci, M. Scarsella, Steam reforming of tar model compounds over ni supported on CeO₂ and mayenite, *Can. J. Chem. Eng.* 95 (2017) 1745–1751, <https://doi.org/10.1002/cjce.22887>.
- [9] W. Torres, S.S. Pansare, J.G. Goodwin, Hot gas removal of tars, ammonia, and hydrogen sulfide from biomass gasification gas, *Catal. Rev. - Sci. Eng.* 49 (2007) 407–456, <https://doi.org/10.1080/01614940701375134>.
- [10] P.E.J. Abbott, N. Macleod, G.E. Wilson, Process For Generating a Synthetic Natural Gas, US2013/0317126 A1 (2013).
- [11] M. Mackles, Process For Desulfurization of Coke Oven Gas, 4,041,130 (1977).
- [12] A. Attar, Chemistry, thermodynamics and kinetics of reactions of sulphur in coal-gas reactions: a review, *Fuel*. 57 (1978) 201–212, [https://doi.org/10.1016/0016-2361\(78\)90117-5](https://doi.org/10.1016/0016-2361(78)90117-5).
- [13] M. Yu, N. Zhang, L. Fan, C. Zhang, X. He, M. Zheng, Z. Li, Removal of organic sulfur compounds from diesel by adsorption on carbon materials, *Int. Rev. Chem. Eng.* 31 (2015) 27–43, <https://doi.org/10.1515/revce-2014-0017>.
- [14] S.L. Lakshapatri, M.A. Abraham, Deactivation due to sulfur poisoning and carbon deposition on Rh-Ni/Al₂O₃ catalyst during steam reforming of sulfur-doped n-hexadecane, *Appl. Catal. A Gen.* 364 (2009) 113–121, <https://doi.org/10.1016/j.apcata.2009.05.035>.
- [15] Y. Lu, J. Chen, Y. Liu, Q. Xue, M. He, Highly sulfur-tolerant Pt/Ce_{0.8}Gd_{0.2}O_{1.9} catalyst for steam reforming of liquid hydrocarbons in fuel cell applications, *J. Catal.* 254 (2008) 39–48, <https://doi.org/10.1016/j.jcat.2007.11.015>.
- [16] S.L. Lakshapatri, M.A. Abraham, Analysis of catalyst deactivation during steam reforming of jet fuel on Ni-(PdRh)/γ-Al₂O₃ catalyst, *Appl. Catal. A Gen.* 405 (2011) 149–159, <https://doi.org/10.1016/j.apcata.2011.08.004>.
- [17] U. Rhyner, P. Edinger, T.J. Schildhauer, S.M.A. Biollaz, Experimental study on high temperature catalytic conversion of tars and organic sulfur compounds, *Int. J. Hydrogen Energy* 39 (2014) 4926–4937, <https://doi.org/10.1016/j.ijhydene.2014.01.082>.
- [18] J.M. Mayne, A.R. Tadd, K.A. Dahlberg, J.W. Schwank, Influence of thiophene on the isoctane reforming activity of Ni-based catalysts, *J. Catal.* 271 (2010) 140–152, <https://doi.org/10.1016/j.jcat.2010.02.018>.
- [19] P.W. Wentreek, J.G. McCarty, C.M. Ablow, H. Wise, Deactivation of alumina-supported nickel and ruthenium catalysts by sulfur compounds, *J. Catal.* 61 (1980) 232–241, [https://doi.org/10.1016/0021-9517\(80\)90359-0](https://doi.org/10.1016/0021-9517(80)90359-0).
- [20] M. Argyle, C. Bartholomew, Heterogeneous catalyst deactivation and regeneration: a review, *Catalysts*. 5 (2015) 145–269, <https://doi.org/10.3390/catal5010145>.
- [21] C.H. Bartholomew, P.K. Agrawal, J.R. Katzer, Sulfur poisoning of metals, *J. Adv. Catal. Sci. Technol.* 31 (1982) 135–242, [https://doi.org/10.1016/S0360-0564\(08\)60454-X](https://doi.org/10.1016/S0360-0564(08)60454-X).
- [22] M. Ashrafi, T. Pröll, C. Pfeifer, H. Hofbauer, Experimental study of model biogas catalytic steam reforming: 2. Impact of sulfur on the deactivation and regeneration of Ni-based catalysts, *Energy Fuels* 22 (2008) 4190–4195, <https://doi.org/10.1021/ef800081j>.
- [23] S. Appari, V.M. Janardhanan, R. Bauri, S. Jayanti, Deactivation and regeneration of Ni catalyst during steam reforming of model biogas: an experimental investigation, *Int. J. Hydrogen Energy* 39 (2014) 297–304, <https://doi.org/10.1016/j.ijhydene.2013.10.056>.
- [24] J. Hepola, P. Simell, Sulphur poisoning of nickel-based hot gas cleaning catalysts in synthetic gasification gas II. Chemisorption of hydrogen sulphide, *Appl. Catal. B Environ.* 14 (1997) 305–321, [https://doi.org/10.1016/S0926-3373\(97\)00030-1](https://doi.org/10.1016/S0926-3373(97)00030-1).
- [25] J.R. Rostrup-Nielsen, L. Christiansen, Concepts in Syngas Manufacture vol. 10, Imperial College Press, London, 2011.
- [26] I. Alstrup, J.R. Rostrup-Nielsen, S. Røen, High temperature hydrogen sulfide chemisorption on nickel catalysts, *Appl. Catal. A* (1981) 303–314, [https://doi.org/10.1016/0166-9834\(81\)80036-X](https://doi.org/10.1016/0166-9834(81)80036-X).
- [27] J. Rostrup-Nielsen, J.R. Anderson, M. Boudart (Eds.), Catalytic Steam Reforming, vol. 5, Springer, Berlin, 1984, pp. 1–117, , https://doi.org/10.1007/978-3-642-93247-2_1 Catal. Sci. Technol.
- [28] P.H. Moud, K.J. Andersson, R. Lanza, K. Engvall, Equilibrium potassium coverage and its effect on a Ni tar reforming catalyst in alkali- and sulfur-laden biomass gasification gases, *Appl. Catal. B Environ.* 190 (2016) 137–146, <https://doi.org/10.1016/j.apcatb.2016.03.007>.
- [29] A. Jess, Catalytic upgrading of tarry fuel gases: a kinetic study with model components, *Chem. Eng. Process. Process Intensif.* 35 (1996) 487–494, [https://doi.org/10.1016/S0255-2701\(96\)04160-8](https://doi.org/10.1016/S0255-2701(96)04160-8).
- [30] J. Hepola, P. Simell, Sulphur poisoning of nickel-based hot gas cleaning catalysts in synthetic gasification gas I. Effect of different process parameters, *Appl. Catal. B Environ.* 14 (1997) 287–303, [https://doi.org/10.1016/S0926-3373\(97\)00031-3](https://doi.org/10.1016/S0926-3373(97)00031-3).
- [31] A. Jess, Mechanisms and kinetics of thermal reactions of aromatic hydrocarbons from pyrolysis of solid fuels, *Fuel*. 75 (1996) 1441–1448, [https://doi.org/10.1016/0016-2361\(96\)00136-6](https://doi.org/10.1016/0016-2361(96)00136-6).
- [32] V. Maurice, N. Kitakatsu, M. Siegers, P. Marcus, Low-coverage sulfur induced reconstruction of Ni(111), *Surf. Sci.* 373 (1997) 307–317, [https://doi.org/10.1016/S0039-6028\(96\)01182-X](https://doi.org/10.1016/S0039-6028(96)01182-X).
- [33] H.S. Bengaard, J.K. Nørskov, J. Sehested, B.S. Clausen, L.P. Nielsen, A.M. Molenbroek, J.R. Rostrup-Nielsen, Steam reforming and graphite formation on Ni catalysts, *J. Catal.* 209 (2002) 365–384, <https://doi.org/10.1006/jcat.2002.3579>.
- [34] M.P. Andersson, F. Abild-Pedersen, I.N. Remediakis, T. Bligaard, G. Jones, J. Engbæk, O. Lytken, S. Horch, J.H. Nielsen, J. Sehested, J.R. Rostrup-Nielsen, J.K. Nørskov, I. Chorkendorff, Structure sensitivity of the methanation reaction: H₂-induced CO dissociation on nickel surfaces, *J. Catal.* 255 (2008) 6–19, <https://doi.org/10.1016/j.jcat.2007.12.016>.
- [35] J. Hepola, J. McCarty, G. Krishnan, V. Wong, Elucidation of behavior of sulfur on nickel-based hot gas cleaning catalysts, *Appl. Catal. B Environ.* 20 (1999) 191–203, [https://doi.org/10.1016/S0926-3373\(98\)00104-0](https://doi.org/10.1016/S0926-3373(98)00104-0).
- [36] J. Hepola, Sulfur Transformations in Catalytic Hot-gas Cleaning of Gasification Gas, VTT Publ., 2000, pp. 1–54.
- [37] T. Ogura, T. Ishimoto, M. Koyama, Density functional theory study of sulfur poisoning on nickel anode in solid oxide fuel cells: effects of surface and subsurface sulfur atoms, *J. Chem. Eng. Japan*. 47 (2014) 793–800, <https://doi.org/10.1252/jcej.12we249>.
- [38] C. Ng, G. Martin, Poisoning of Ni/SiO₂ catalysts with H₂S: chemisorption of H₂, CO, C₆H₆, and C₂H₂ studied by magnetic methods, *J. Catal.* 54 (1978) 384–396, [https://doi.org/10.1016/0021-9517\(78\)90086-6](https://doi.org/10.1016/0021-9517(78)90086-6).
- [39] S. Weeks, E. Plummer, New evidence for multiple binding sites for sulfur at the Ni (100)-vacuum interface, *Chem. Phys. Lett.* 48 (1977) 601–603, [https://doi.org/10.1016/0009-2614\(77\)85103-8](https://doi.org/10.1016/0009-2614(77)85103-8).
- [40] A. Grossmann, W. Erley, H. Ibach, Adsorbate-induced surface stress and surface reconstruction: oxygen, sulfur and carbon on Ni(111), *Surf. Sci.* 337 (1995) 183–189, [https://doi.org/10.1016/0039-6028\(95\)00615-X](https://doi.org/10.1016/0039-6028(95)00615-X).
- [41] L. Ruan, I. Stensgaard, F. Besenbacher, E. Laegsgaard, Observation of a Missing-Row Structure on an fcc (111) Surface : The (5√3 X 2) S Phase on Ni (111) Studied by Scanning Tunneling Microscopy, *Phys. Rev. Lett.* 71 (1993), <https://doi.org/10.1103/PhysRevLett.71.2963>.
- [42] J.R. Rostrup-nielsen, Chemisorption of hydrogen sulfide on a supported nickel catalyst, *J. Catal.* 11 (1968) 220–227, [https://doi.org/10.1016/0021-9517\(68\)90035-3](https://doi.org/10.1016/0021-9517(68)90035-3).
- [43] Y. Chen, C. Xie, Y. Li, C. Song, T.B. Bolin, Sulfur poisoning mechanism of steam reforming catalysts: an X-ray absorption near edge structure (XANES) spectroscopy study, *Phys. Chem. Chem. Phys.* 12 (2010) 5503–5513, <https://doi.org/10.1039/b926434e>.
- [44] E.B. Maxted, The poisoning of metallic catalysts, *J. Adv. Catal. Sci. Technol.* 3 (1951) 129–178, [https://doi.org/10.1016/S0360-0564\(08\)60106-6](https://doi.org/10.1016/S0360-0564(08)60106-6).
- [45] K. Lee, E. Lee, C. Song, M.J. Janik, Density functional theory study of propane steam reforming on Rh-Ni bimetallic surface: sulfur tolerance and scaling/Br??Nsted-Evans-Polanyi relations, *J. Catal.* 309 (2014) 248–259, <https://doi.org/10.1016/j.jcat.2013.10.006>.
- [46] J.A. Rodriguez, J. Hrbek, Interaction of sulfur with well-defined metal and oxide surfaces: unraveling the mysteries behind catalyst poisoning and desulfurization, *Acc. Chem. Res.* 32 (1999) 719–728, <https://doi.org/10.1021/ar9801191>.
- [47] F. Abild-Pedersen, O. Lytken, J. Engbæk, G. Nielsen, I. Chorkendorff, J.K. Nørskov, Methane activation on Ni(1 1 1): effects of poisons and step defects, *Surf. Sci.* 590 (2005) 127–137, <https://doi.org/10.1016/j.susc.2005.05.057>.
- [48] C. Karakaya, R. Ottersatter, L. Maier, O. Deutschmann, Kinetics of the water-gas shift reaction over Rh/Al₂O₃catalysts, *Appl. Catal. A Gen.* 470 (2014) 31–44, <https://doi.org/10.1016/j.apcata.2013.10.030>.

- [49] R. Chakrabarti, J.L. Colby, L.D. Schmidt, Effects of biomass inorganics on rhodium catalysts: I. Steam methane reforming, *Appl. Catal. B Environ.* 107 (2011) 88–94, <https://doi.org/10.1016/j.apcatb.2011.06.040>.
- [50] S. Peucheret, M. Feaviour, S. Golunski, Exhaust-gas reforming using precious metal catalysts, *Appl. Catal. B Environ.* 65 (2006) 201–206, <https://doi.org/10.1016/j.apcatb.2006.01.009>.
- [51] M.P. Andersson, F. Abild-Pedersen, I.N. Remediakis, T. Bligaard, G. Jones, J. Engbæk, O. Lytken, S. Horch, J.H. Nielsen, J. Sehested, J.R. Rostrup-Nielsen, J.K. Nørskov, I. Chorkendorff, Structure sensitivity of the methanation reaction: H₂-induced CO dissociation on nickel surfaces, *J. Catal.* 255 (2008) 6–19, <https://doi.org/10.1016/j.jcat.2007.12.016>.
- [52] C. Li, D. Hirabayashi, K. Suzuki, A crucial role of O²⁻ and O₂²⁻ on mayenite structure for biomass tar steam reforming over Ni/Ca₁₂Al₁₄O₃₃, *Appl. Catal. B Environ.* 88 (2009) 351–360, <https://doi.org/10.1016/j.apcatb.2008.11.004>.
- [53] C.R. Müller, R. Pacciani, C.D. Bohn, S.A. Scott, J.S. Dennis, Investigation of the enhanced water gas shift reaction using natural and synthetic sorbents for the capture of CO₂, *Ind. Eng. Chem. Res.* 48 (2009) 10284–10291, <https://doi.org/10.1021/ie900772q>.
- [54] P. Yrjas, K. Iisa, M. Hupa, Limestone and dolomite as sulfur absorbents under pressurized gasification conditions, *Fuel* 75 (1996) 89–95, [https://doi.org/10.1016/0016-2361\(95\)00204-9](https://doi.org/10.1016/0016-2361(95)00204-9).
- [55] C.A.P. Zevenhoven, K.P. Yrjas, M.M. Hupa, Hydrogen sulfide capture by limestone and dolomite at elevated pressure. 2. Sorbent particle conversion modeling, *Ind. Eng. Chem. Res.* 35 (1996) 943–949, <https://doi.org/10.1021/ie950539j>.
- [56] J.R. Rostrup-nielsen, Some principles relating to the regeneration of sulfur-poisoned nickel catalysts, *J. Catal.* 21 (1971) 171–178, [https://doi.org/10.1016/0021-9517\(71\)90135-7](https://doi.org/10.1016/0021-9517(71)90135-7).
- [57] M. Hartman, K. Svoboda, O. Trnka, J. Čermák, Reaction between hydrogen sulfide and limestone calcines, *Ind. Eng. Chem. Res.* 41 (2002) 2392–2398, <https://doi.org/10.1021/ie010805v>.
- [58] A.B.M. Heesink, W.P.M. Van Swaaij, The sulphidation of calcined limestone with hydrogen sulphide and carbonyl sulphide, *Chem. Eng. Sci.* 50 (1995) 2983–2996, [https://doi.org/10.1016/0009-2509\(95\)91133-J](https://doi.org/10.1016/0009-2509(95)91133-J).